Research on Engineering Structures & Materials
www.jresm.org
MIM Research Group

Research Article

Flexural fatigue performance of ternary blended geopolymer concrete

Mudiyam Deepthi [*,a], M. Sri Murali [b]

Department of Civil Engineering, Sri Venkateshwara University College of Engineering, Tirupati, Andhra Pradesh, India

Article Info

Article History:

Received 19 May 2026

Accepted 06 Oct 2026

Keywords:

Fatigue Life;
Endurance limit;
Weibull distribution;
Concrete beams;
S–N curve;
Flexural fatigue

Abstract

Fatigue behavior of geopolymer concrete (GPC) is important for pavement and structural systems subjected to repeated loading. This study investigates the fatigue performance of modified geopolymer concrete by examining the effects of activator molarity and material modifications using fly ash (FA), alccofine (AF), nano-silica (NS), I-Crete, and banana fiber (BF). Six geopolymer concrete mixtures were developed using 90% FA and 10% AF. The control mixtures were prepared with 8, 10, and 12 M NaOH and sodium silicate (Na_2SiO_3), while the modified mixtures incorporated 2% nano-silica, 2% I-Crete, and 2% banana fiber at 12 M NaOH. Fatigue loading tests were conducted on beam specimens (100 mm × 100 mm × 500 mm) at a frequency of 2 Hz and stress levels of 0.8 and 0.9. Fatigue behavior was evaluated using two-parameter Weibull analysis and reliability-based design fatigue-life assessment. The Weibull parameters increased with increasing activator molarity and material modification, particularly at a stress level of 0.8. Material modifications improved fatigue resistance, with banana-fiber-modified geopolymer concrete exhibiting the highest fatigue performance. At a failure probability of 0.01, the design fatigue life ranged from 2,184 to 4,831 cycles, while at a failure probability of 0.05, it ranged from 3,147 to 6,335 cycles. The endurance limit after 2 million loading cycles remained relatively stable, ranging from 49.0% to 50.5% of the flexural strength. Overall, increasing activator molarity and incorporating material modifications enhanced the fatigue resistance of geopolymer concrete, with banana fiber providing the most pronounced improvement.

© 2026 MIM Research Group. All rights reserved.

1. Introduction

Concrete is one of the most widely used construction materials, but the manufacture of ordinary Portland cement (OPC) results in significant CO_2 emissions and environmental impacts [1,2]. To reduce these environmental effects, GPC has become a sustainable alternative that uses aluminosilicate-rich materials such as FA, ground granulated blast furnace slag (GGBS), and metakaolin to produce a polymeric binder through geopolymerization via activation with alkaline solutions [3]. In addition to being more sustainable, GPC exhibits superior mechanical properties, including increased strength, durability and resistance to degradation in harsh environments [4,5].

Concrete members are subject to cyclic loads and stresses when used in structural and pavement applications, which, in turn, lead to the initiation and propagation of cracks and ultimately to fatigue failure. Fatigue performance is an important consideration in estimating the life expectancy of concrete structures. It has been found that GPC has demonstrated flexural strength and fatigue behavior comparable to, or better than, those of traditional OPC concrete, largely due to its compact microstructure and strong binding matrix [6,7]. Although these have benefits, the flexural fatigue

*Corresponding author: m.deepthiphd@gmail.com
[a]orcid.org/0009-0005-7904-8748; [b]orcid.org/0000-0002-6901-9442
DOI: http://dx.doi.org/10.17515/resm2026-1694me0519rs

behavior of GPC has not been researched extensively, especially under different loading conditions. Therefore, additional research is needed to deepen the understanding of its fatigue performance and ensure its reliability in applications to rigid pavements and structural components.

Previous studies have demonstrated the potential of GPC for applications subjected to repeated loading. Deivabalan and Saravanan [8] investigated the fatigue behavior of FA-based geopolymer concrete beams and evaluated the response using S–N relationships [20] investigated the flexural fatigue behavior of FA-based GPC under sulphate attack and demonstrated that environmental deterioration can influence its fatigue performance. More recently [21] investigated the fatigue performance of paving-grade GPC incorporating slag sand. Their results showed improved fatigue endurance with slag sand incorporation, and the fatigue data were evaluated using S–N and probabilistic approaches.

Fibre incorporation is another promising approach for improving the fatigue resistance and crack-control capability of GPC [22] investigated steel-fibre-reinforced GPC under cyclic loading and reported substantially higher fatigue resistance than unreinforced concrete, with the addition of steel fibres producing a significant improvement in fatigue life [23] investigated the flexural fatigue behavior of GPC containing modified basalt and PVA fibres. Their results showed that hybrid fibres effectively restrained crack initiation and propagation and improved fatigue performance. However, existing fatigue studies on fibre-reinforced GPC have predominantly focused on steel, basalt and PVA fibres. The fatigue behavior of GPC incorporating alternative fibre types, particularly BF, remains insufficiently explored. Fatigue life is inherently associated with considerable variability because concrete is a quasi-brittle heterogeneous material. Consequently, evaluation based only on average fatigue life or deterministic S–N relationships may not adequately represent the reliability of concrete under repeated loading [24] demonstrated that flexural fatigue life exhibits substantial dispersion and employed a two-parameter Weibull distribution to establish probabilistic fatigue equations at different survival levels. Their results showed that Weibull analysis can effectively describe the variability of fatigue-life data and provide a reliability-based assessment of fatigue performance. [23] Similarly, they confirmed that the fatigue lives of fibre-reinforced GPC followed a two-parameter Weibull distribution, while [21] applied probabilistic analysis to paving-grade GPC fatigue data.

Despite these advances, several research gaps remain. First, the available studies on the flexural fatigue behavior of GPC are relatively limited compared with conventional concrete. Second, existing fiber-reinforced GPC fatigue studies have mainly concentrated on steel, basalt and PVA fibers, with limited attention to alternative fibres such as BF. Third, although Weibull-based models have been applied to concrete and GPC fatigue data, limited studies have systematically combined variations in activator molarity with different material modifications and reliability-based fatigue-life assessment. In particular, the effects of NaOH molarity together with nano-silica, I-Crete and BF modifications on the flexural fatigue behavior of GPC have not been adequately established.

Therefore, the present study investigates the flexural fatigue behavior of modified GPC by considering different NaOH molarities and material modifications involving NS, I-Crete and BF. Six GPC mixtures are experimentally evaluated under repeated flexural loading at different stress levels. The fatigue-life data are analyzed using a two-parameter Weibull distribution to quantify fatigue-life variability, failure probability and reliability-based design fatigue life. The study aims to establish the influence of activator molarity and material modifications on the fatigue resistance and reliability of GPC and to identify the mixture exhibiting the most favorable fatigue performance for potential pavement and structural applications.

1.1 Innovation of the Research

The present study addresses the limited research on the flexural fatigue behavior of sustainable GPC incorporating FA, AF, NS, I-Crete, and BF in a combined system. Unlike previous studies, which mainly focused on conventional or individually modified geopolymer concrete, this study investigates their combined influence on mechanical and flexural fatigue performance at different NaOH molarities (8M, 10M and 12M). The study identifies the optimum material combination and alkaline activator molarity and evaluates its fatigue life, endurance, and failure behavior under

stress levels of 0.80 and 0.90 at a loading frequency of 2 Hz. The findings provide new insights into the potential application of sustainable GPC in structural components subjected to repeated loading.

Table 1. Notation and description of parameters used in the study

Symbol	Description
α	Shape parameter
σ	Standard deviation
Γ	Gamma function
μ	Mean value
u	Scale parameter (characteristic life)
CoV	Coefficient of variation
fmax	Maximum fatigue stress
fmin	Minimum fatigue stress
fr	Static flexural strength
L_N	Survival probability
N	Cycles to failure
N_D	Design fatigue life
P_f	Probability of failure
R	Stress ratio (fmin/fmax)
S	Stress level

2. Materials Used

The materials used in the preparation of geopolymer concrete (GPC) mixtures included fly ash (FA), alccofine (AF), coarse aggregate (CA), sodium hydroxide (NaOH), sodium silicate (Na_2SiO_3), nano-silica (NS), I-Crete, and banana fibre (BF). Fly ash was collected from a thermal power plant located in Vijayawada, Andhra Pradesh, India. Alccofine, sodium hydroxide, sodium silicate, and nano-silica were procured from Herenba Instrument and Engineering, Chennai, Tamil Nadu, India. Coarse and fine aggregates were obtained from locally available quarries in Nandyal district, Andhra Pradesh, India. I-Crete was procured from Navodya Company, Chennai, Tamil Nadu, India, while banana fibre was obtained from Herenba Instrument and Engineering, Chennai, Tamil Nadu, India. All the materials were tested in accordance with IS 383:2016 [25] and the relevant MoRTH specifications. Natural coarse aggregate (NCA) 20 mm and fine aggregate (FA) Zone II sand were used in this study. The NCA had a specific gravity of 2.84 and a bulk density of 1800 kg/m^3. In addition, it exhibited impact values of 18.96%, crushing values of 18.01%, and water absorption of 0.30%, confirming its suitability for concrete. The FA satisfied Zone II grading requirements, ensuring proper particle distribution. Sieve analysis also confirmed the suitability of both aggregates for mix design. Table 2 presents the chemical composition of FA, I-Crete, and AF.

FA was used as the primary binder. The alkaline activating solution consisted of NaOH and Na_2SiO_3, with NaOH concentrations of 8 M, 10 M, and 12 M. All materials satisfied the required standards and were used for GPC preparation. Table 3 presents the mix proportions.

Table 2. Chemical composition of FA, I-Crete, and AF-1203

Chemical Composition	FA (%)	I-Crete (%)	AF- 1203
C	23.29	23.52	-
CaO	3.10	3.13	32.30
SiO_2	36.10	36.46	35.30
Al_2O_3	25.03	25.28	21.40
Fe_2O_3	8.66	8.75	1.20
MgO	1.24	1.25	6.20
Na_2O	0.0	0.0	-
SO_3	0.59	0.6	0.13
TiO_2	-	0.92	-

2.1 Sample Preparation and Test

GPC mixtures were prepared at different molarities and with various material modifications to evaluate their performance. Mixtures M1, M2, and M3 contained 90% FA and 10% AF, respectively, with NaOH and Na_2SiO_3 molarity levels of 8 M, 10 M, and 12 M, respectively. In all mixtures, the activating solution was prepared with NaOH and Na_2SiO_3, with the NaOH concentration varied and the amount of sodium silicate kept constant. To study the effect of additional materials, M4, M5, and M6 were developed based on the M3 mixture (12 M). Mixture M4 contained 2% NS, M5 contained 2% I-Crete, and M6 contained 2% BF. These variations were introduced to analyze the effects of molarity and associated additives on GPC properties.



Fig. 1. Flexural fatigue test setup and failure specimens

The alkaline activator consisted of NaOH and Na_2SiO_3 solutions. NaOH pellets were dissolved in distilled water to the required molarity and allowed to cool for 24 h due to the exothermic dissolution. Na_2SiO_3 was then added and mixed thoroughly. The activator promotes dissolution of reactive silica and alumina in FA and AF, facilitating geopolymerization. It was gradually added during mechanical mixing. The total alkaline solution was 167.0 kg/m^3, comprising 66.8 kg/m^3 NaOH and 100.2 kg/m^3 Na_2SiO_3, with an alkaline solution-to-binder ratio of 0.45.

2.2 Experimental Methodology

The experimental investigation was carried out in two stages.

2.2.1 Static Flexural Test

Beam specimens of 100 × 100 × 500 mm were cured for 90 days as per the curing period followed in accordance with IRC:58[26] and then tested under static flexural loading. Three specimens were

tested for each mix, and the average maximum load was considered to determine the representative peak load. The load–deflection curves were plotted using the average values. The average peak load obtained from the static test was used to determine the maximum and minimum loads for the subsequent fatigue test at the specified stress ratio. The experimental setup is shown in Fig. 1.

2.2.2 Flexural Fatigue Test

Based on the average static peak load, the maximum fatigue load was determined for the selected stress level, and the minimum load was calculated using the stress ratio (R = 0.10). The specimens were subjected to repeated flexural loading at a frequency of 2 Hz until failure. The corresponding number of loading cycles was recorded as the fatigue life. For each stress level and mixture, fatigue tests were performed on four specimens. The number of specimens was limited considering the time-consuming nature of fatigue testing and to maintain a cost-effective experimental program.

Table 3. Mix proportions

Mix ID	Mix designations	FA	AF	NS	I-Crete	BF
M1	MFA90AF10	333.99	37.11	0	0	0
M2	MFA90AF10	333.99	37.11	0	0	0
M3	MFA90AF10	333.99	37.11	0	0	0
M4	MFA90AF10N2	333.99	37.11	7.42	0	0
M5	MFA90AF10IC2	333.99	37.11	0	7.42	0
M6	MFA90AF10BF2	333.99	37.11	0	0	7.42

Mix ID	FA	CA	Molarity	Total Alkalinity Solution	NaOH	Na_2SiO_3
M1	704.37	1257.73	8M	167	66.8	100.2
M2	704.37	1257.73	10M	167	66.8	100.2
M3	704.37	1257.73	12M	167	66.8	100.2
M4	704.37	1257.73	12M	167	66.8	100.2
M5	704.37	1257.73	12M	167	66.8	100.2
M6	704.37	1257.73	12M	167	66.8	100.2

3. Load-Deflection Curve

The average of three specimens tested after 90 days of curing was considered to ensure the reliability of the results. During flexural testing, the specimens were subjected to the adopted loading procedure, and the corresponding load and deflection were recorded in accordance with the testing procedure reported in previous literature [8], load–deflection behavior was recorded, and load–deflection curves were plotted using the average values from the three specimens, as shown in Fig. 2. These curves were used to determine the ultimate load and to establish the appropriate stress levels for subsequent fatigue testing. Table 4 presents the loading parameters for the fatigue test, including the minimum and maximum load values. Table 5 presents the fatigue life-to-failure (N) obtained from laboratory tests, including the number of cycles recorded for each specimen.

3.1 Load–Deflection and Hysteresis Behavior

The load–deflection curves show an initial nearly linear response, indicating the elastic behavior of the mixes. Differences in the initial slopes indicate variations in stiffness. With increasing load, the

curves become nonlinear due to crack initiation and propagation. The peak load varies among the mixes. M6 shows the highest peak load, 14.5 kN, followed by M4 12.5 kN, while M1 and M5 reach approximately 12 kN. After the peak load, a gradual reduction in load is observed, indicating the post-cracking response and residual load-carrying capacity. The hysteresis curves show repeated loading and unloading behavior under cyclic loading. The enclosed hysteresis loops indicate energy dissipation, while the progressive change in loop shape reflects stiffness degradation and accumulation of damage with increasing cycles. The relatively wider loops indicate greater deformation and energy dissipation. The incorporation of NS, I-Crete and BF influences stiffness, peak load and post-cracking behavior by modifying the concrete matrix and crack propagation characteristics. Fig. 3 shows the hysteresis curves for M1–M6 mixes under cyclic loading at a stress level of 0.80.

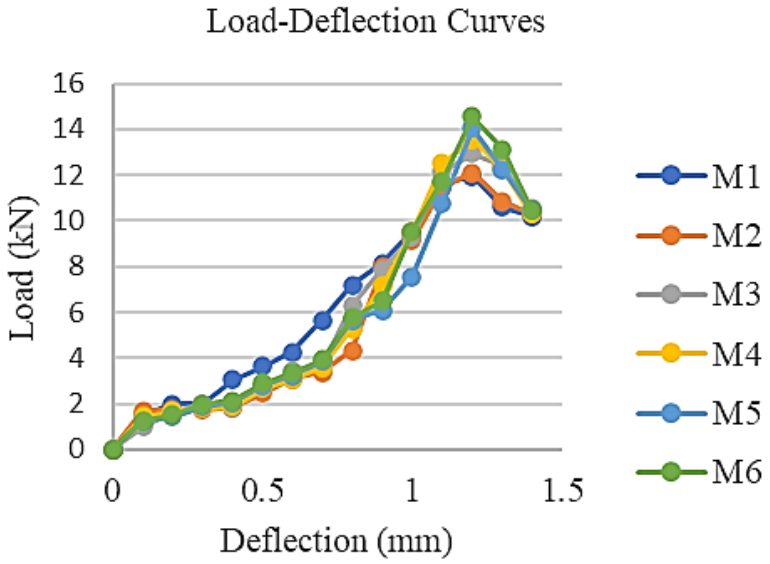
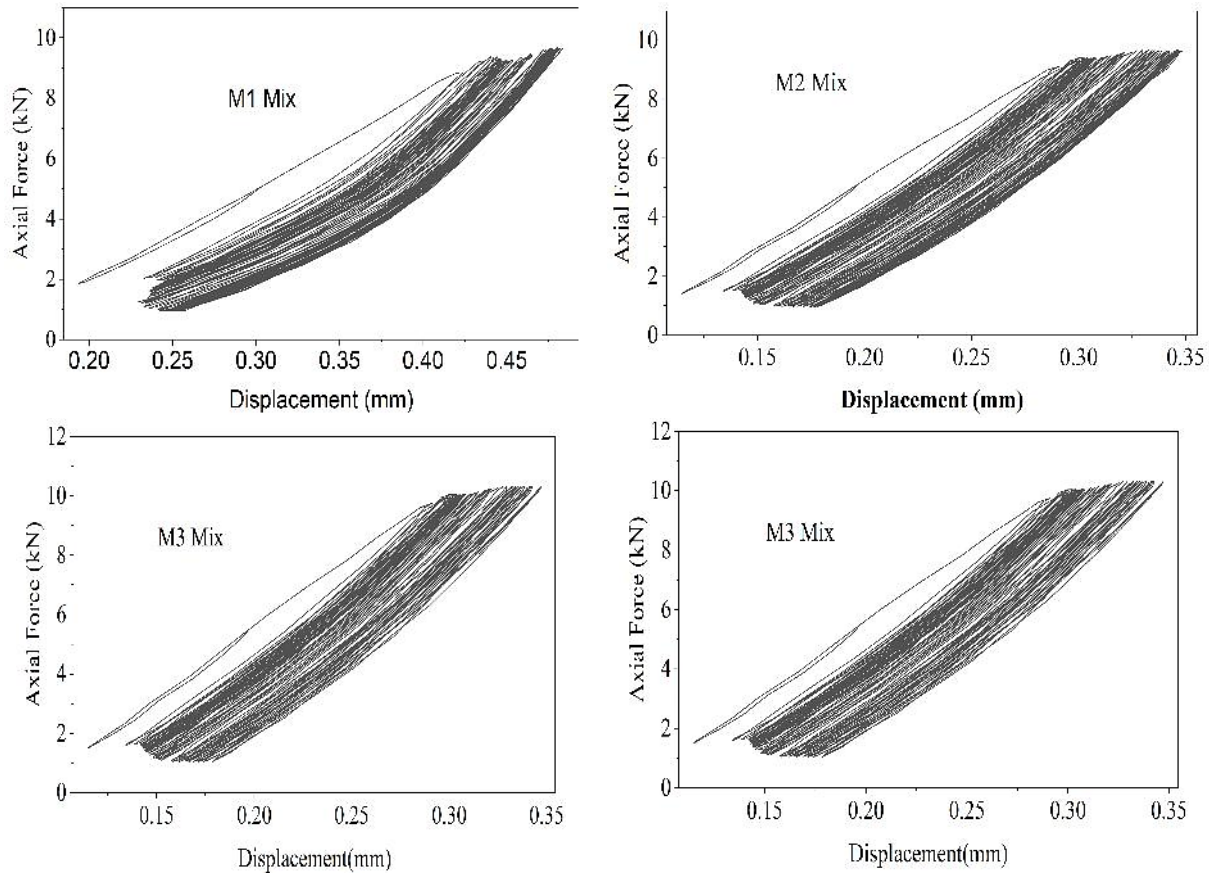


Fig. 2. Load–deflection curves of various mixes under static flexural loading



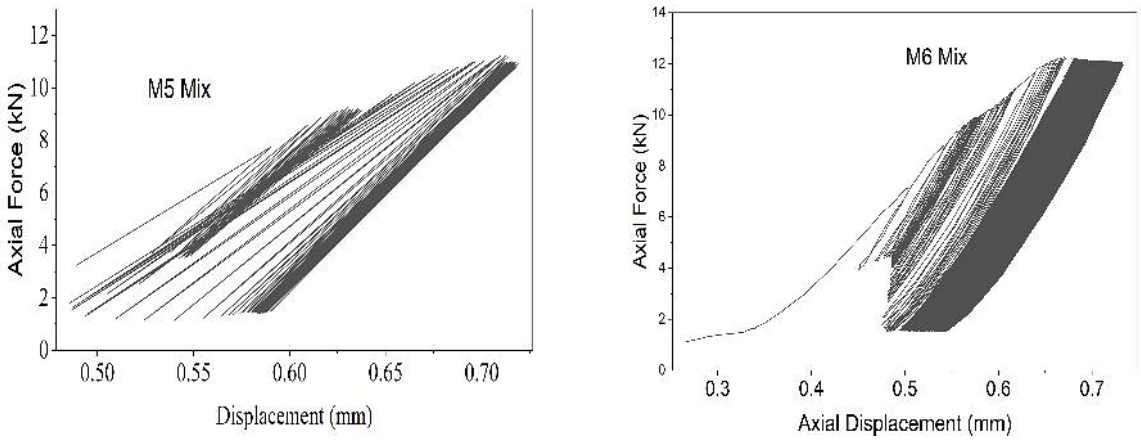


Fig. 3. Hysteresis curves for M1-M6 Mix under cyclic loading at a stress level of 0.80

3.2 Crack Pattern and Failure Behavior

The specimens primarily exhibit flexural cracking in the tensile region, followed by crack propagation towards the compression zone. With continued loading, the dominant crack widens and ultimately leads to failure. The differences in post-cracking response among the mixes indicate variations in crack propagation and residual load-carrying capacity. BF can contribute to crack bridging and restriction of crack opening, while NS and I-Crete can improve the matrix and interfacial characteristics. These effects influence the cracking and failure behavior and consequently the fatigue performance.

Table 4. Loading parameters for fatigue test

Mix ID	Peak load (kN)	Stress level=0.80		Stress level=0.90	
		P_{max} (kN)	P_{min} (kN)	P_{max} (kN)	P_{min} (kN)
M1	11.56	9.24	0.924	10.40	1.040
M2	12.10	9.68	0.968	10.89	1.089
M3	12.95	10.36	1.036	11.65	1.165
M4	13.05	10.44	1.044	11.74	1.174
M5	14.05	11.24	1.124	12.64	1.264
M6	14.55	11.64	1.164	13.09	1.309

Table 5. Fatigue life failure (N) Laboratory test

Mix ID	Fatigue life(N)					
	M1	M2	M3	M4	M5	M6
Stress level=0.80	7090	7400	7950	8320	8750	9550
	8250	8690	9500	9316	9999	10560
	9600	9900	10602	10660	11103	11809
	9820	10099	11000	11156	11650	12700
Stress level=0.90	1270	1390	1410	1495	1525	1830
	1501	1680	1750	1790	1860	2060
	1740	1990	2001	2056	2105	2330
	1830	2035	2100	2140	2180	2535

4. Fatigue Result Analysis

4.1 Weibull Distribution in Fatigue Analysis

A two-parameter Weibull distribution is used to examine how the fatigue life of concrete samples differs at a certain stress level. Previous research has identified this distribution as a reliable and efficient model for fatigue-life analysis [9-12]. This study employs a two-parameter Weibull

distribution to assess the fatigue life characteristics of various concrete mixes (M1–M6), utilizing distribution parameters derived from the associated S–N relationships. To determine whether the Weibull model holds, a graphical method is used across various stress levels (S) based on previous studies. The probability density function (PDF) for a two-parameter Weibull distribution is expressed as follows [11,20].

$$f(n)=(\alpha/u)(n/u)^{\alpha}\text{-}1)exp(-(n/u)^{\alpha}) \quad (1)$$

Here, n represents the number of cycles leading to failure. The graphical plots showed an approximately linear relationship between the transformed fatigue life data at the investigated stress levels, indicating that the experimental fatigue-life data could be represented by the two-parameter Weibull distribution. The Weibull parameters obtained from the graphical method were subsequently used to evaluate the fatigue-life distribution and failure probability of the tested mixes. All Notation and descriptions of Parameters Used in the study are presented in Table 1.

4.1.1 Evaluation of Fatigue Life Data Using a Graphical Approach

The graphical method shows that a two-parameter Weibull distribution can be used to describe the fatigue life of concrete at a certain stress level, as shown in Equation (2) [9,11]. In this method, fatigue data are converted into a linear form to verify the applicability of the Weibull model. Following earlier research, the same approach is adopted in the present study for multiple mixes (M1–M6).

The reliability function, expressed in terms of $L_N(N)$, can be represented as follows [9-12].

$$L_N(N) = exp\,[(n/u)^{\alpha}] \quad (2)$$

In this case, n is the specific value of the random variable N. α is the shape parameter for a particular stress level (S), and u is the characteristic life for the same particular stress level. Determine the two-parameter Weibull distribution's α and u using a fatigue test through a graphical approach. This method involves drawing a plot between Y = ln[ln(1/LN)]and X = ln(N). This is the number of cycles to failure at a given stress level (experimentally determined). The fatigue life test results for stress levels 0.80 and 0.90 are presented in Tables 6 and 7. The linear relationship in this plot justifies the use of the Weibull distribution to model fatigue [12]. By applying a double-logarithmic transformation to the survivorship function, the equation can be converted to a linear form (2).

$$ln[ln(1/L_N)] = \alpha\, ln(N) - \alpha\, ln(u) \quad (3)$$

$$Yielding\ Equation\ Y = \alpha X - \eta \quad (4)$$

$$where\ \eta = \alpha\, ln(u) \quad (5)$$

The fatigue life data are first sorted in ascending order of cycles to failure, and then the empirical survivorship function is determined by

$$L_N = i/(k+1) \quad (6)$$

In the above equation, i is the rank of failure, while k is the number of fatigue cycles at a given stress level (S). If the plot of Y = ln[ln(1/LN)]versus X = ln(N) results in a straight line, it suggests that the Weibull distribution is suitable for modeling the fatigue behavior of concrete. The best-fit line is determined by least-squares regression. The slope of the line is used for estimating the shape parameter (α), and the scale parameter (u) is calculated from Equation (5). The values of L_N calculated using Equation (6) for stress ratios of 0.80 and 0.90 are given in Tables 6 and 7, respectively. The values of α and u, as determined graphically, are shown in Tables 8 and 9 and in Fig. 4(a-f) Y = ln[ln(1/LN)]. The analysis is presented in Tables 5 and 6 for stress level ratios of 0.80 and 0.90.

4.1.2 Estimation of Distribution Parameters Using the Method of Moments

The aim of this section is to evaluate the fatigue-life data of mixes M1–M6 using the graphical approach and to verify the suitability of the two-parameter Weibull distribution at stress levels of 0.80 and 0.90. The analysis is used to determine the Weibull shape parameter (α) and characteristic life (u) from the experimental fatigue-life data and thereby characterize the variation in fatigue life and failure probability of the tested mixes. The shape (α) and scale (u) parameters can also be calculated from the following formulae [10,12].

Table 6. Fatigue life data analysis for six types of concrete for stress level 0.80

Mix ID	Failure specimens In ascending order	Ln(N)	Log(N)	L_N=1–(i/(K+1))	ln[ln(1/L_N)]
M1	1	8.86	3.85	0.750	-1.245
	2	9.02	3.91	0.500	-0.366
	3	9.16	3.98	0.250	0.3266
	4	9.19	3.99	0.200	0.475
M2	1	8.90	3.86	0.750	-1.245
	2	9.06	3.93	0.500	-0.366
	3	9.20	3.99	0.250	0.3266
	4	9.22	4.00	0.200	0.475
M3	1	9.11	3.96	0.750	-1.245
	2	9.19	3.99	0.500	-0.366
	3	9.29	4.03	0.250	0.3266
	4	9.32	4.04	0.200	0.475
M4	1	9.11	3.96	0.750	-1.245
	2	9.19	3.99	0.500	-0.366
	3	9.21	4.00	0.250	0.3266
	4	9.31	4.04	0.200	0.475
M5	1	9.11	3.95	0.750	-1.245
	2	9.21	3.99	0.500	-0.366
	3	9.31	4.04	0.250	0.326
	4	9.35	4.06	0.200	0.475
M6	1	9.13	3.96	0.750	-1.245
	2	9.25	4.01	0.500	-0.366
	3	9.37	4.07	0.250	0.326
	4	9.44	4.10	0.200	0.475

Table 7. Fatigue life analysis for four types of concrete. For stress level 0.90

Mix ID	Specimen Numbers	Ln(N)	Log(N)	LN=1-(i/(K+1))	ln[ln(1/ LN)]
M1	1	7.24	3.14	0.750	-1.245
	2	7.36	3.19	0.500	-0.366
	3	7.48	3.25	0.250	0.326
	4	7.51	3.26	0.200	0.475
M2	1	7.43	3.23	0.750	-1.245
	2	7.52	3.26	0.500	-0.366
	3	7.59	3.29	0.250	0.326
	4	7.61	3.30	0.200	0.475
M3	1	7.55	3.27	0.750	-1.245
	2	7.59	3.29	0.500	-0.366
	3	7.64	3.32	0.250	0.326
	4	7.65	3.32	0.200	0.475
M4	1	7.55	3.27	0.750	-1.245
	2	7.59	3.29	0.500	-0.366
	3	7.69	3.34	0.250	0.326
	4	7.75	3.36	0.200	0.475
M5	1	7.54	3.27	0.750	-1.245
	2	7.60	3.27	0.500	-0.366
	3	7.65	3.32	0.250	0.326
	4	7.66	3.32	0.200	0.475
M6	1	7.58	3.29	0.750	-1.245
	2	7.68	3.33	0.500	-0.366
	3	7.79	3.38	0.250	0.326
	4	7.83	3.40	0.200	0.475

$$\alpha = (COV)^{-1.08} \quad (7)$$

$$u = \mu / \Gamma(1+1/\alpha) \quad (8)$$

In this equation, μ is the mean of the fatigue life data at a given stress level, and the coefficient of variation (COV = σ/μ) (where σ is the standard deviation) is a measure of the spread of the data. Γ is the gamma function. The constants α and u, determined by the method of moments, are given in Tables 8 and 9 for stress levels of 0.8 and 0.90.

Tables 5 and 6 indicate a clear reduction in fatigue life with increasing stress level, demonstrating the significant effect of stress level on fatigue performance. The results further show that the material modifications improved the fatigue resistance of the concrete mixes. The consistent trend observed among the specimens indicates reliable fatigue behavior under repeated flexural loading. Overall, the modified mixes demonstrated better capability to withstand cyclic loading, particularly at the lower stress level.

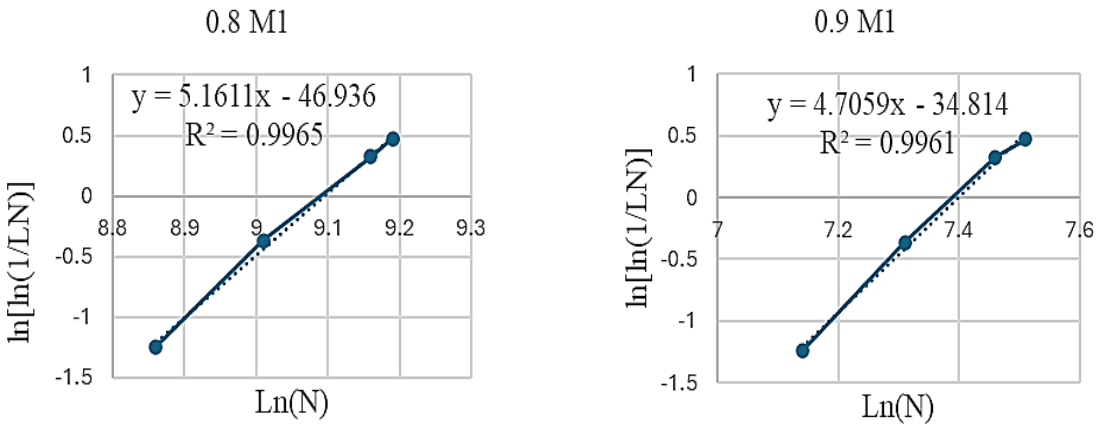
Table 8. Weibull distribution parameter (α, u) for 0.80 stress level

Stress level	Mix ID	Weibull distribution parameters (0.8 stress level)		
		Methods	α	u
0.80	M1	GM	5.161	8902
		MM	7.930	9210
		Average	6.545	9056
		GM	5.299	9265
	M2	MM	8.625	9524
		Average	6.962	9395
	M3	GM	5.482	10347
		MM	8.296	9997
		Average	6.889	10172
		GM	5.853	10067
	M4	MM	8.908	10410
		Average	7.380	10239
	M5	GM	6.122	10626
		MM	9.367	10907
		Average	7.744	10767
		GM	6.253	11385
	M6	MM	9.874	11725
		Average	8.063	11555

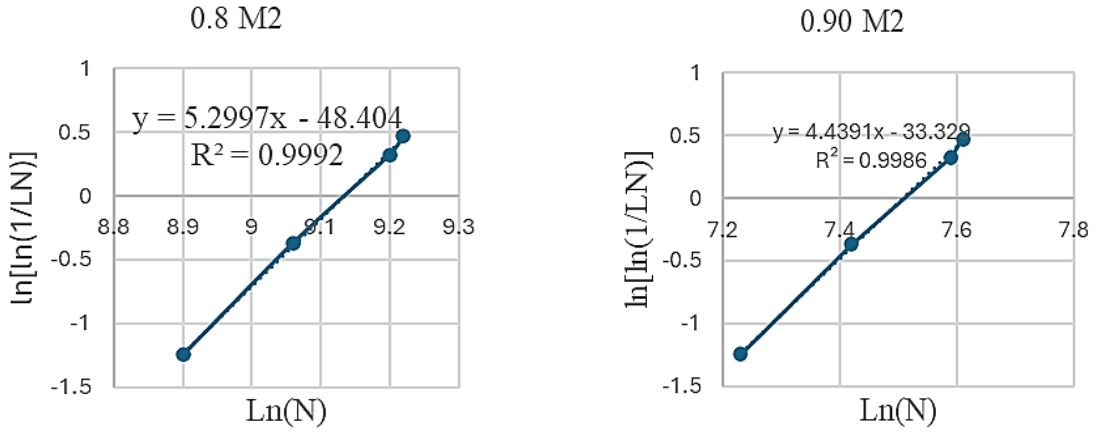
GM = Graphical Method; MM = Method of Moments

Table 9. Weibull distribution parameters (α, u) for 0.90 stress

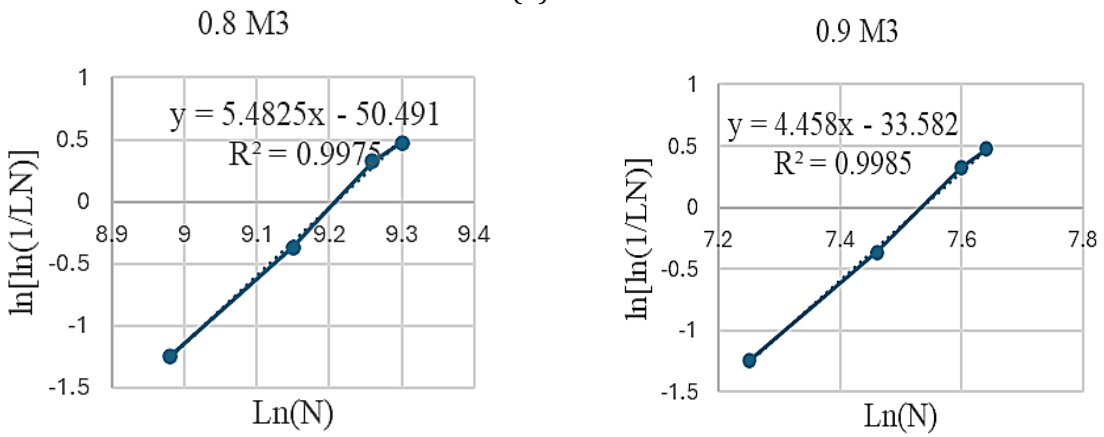
Stress level	Mix ID	0.90 stress Level	α	u
0.90	M1	GM	4.705	1635
		MM	7.140	1733
		Average	5.922	1684
		GM	4.439	1823
	M2	MM	6.693	1895
		Average	5.566	1859
	M3	GM	4.458	1867
		MM	6.529	1947
		Average	5.493	1907
		GM	4.825	1916
	M4	MM	6.955	1998
		Average	5.890	1957
	M5	GM	4.904	1957
		MM	7.336	2041
		Average	6.120	1999
		GM	5.511	2231
	M6	MM	8.232	2320
		Average	6.871	2276



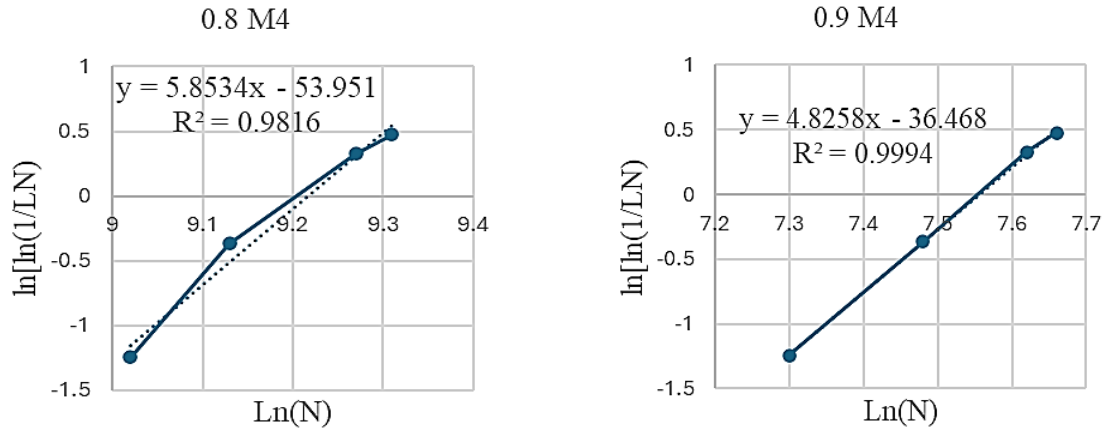
(a) M1



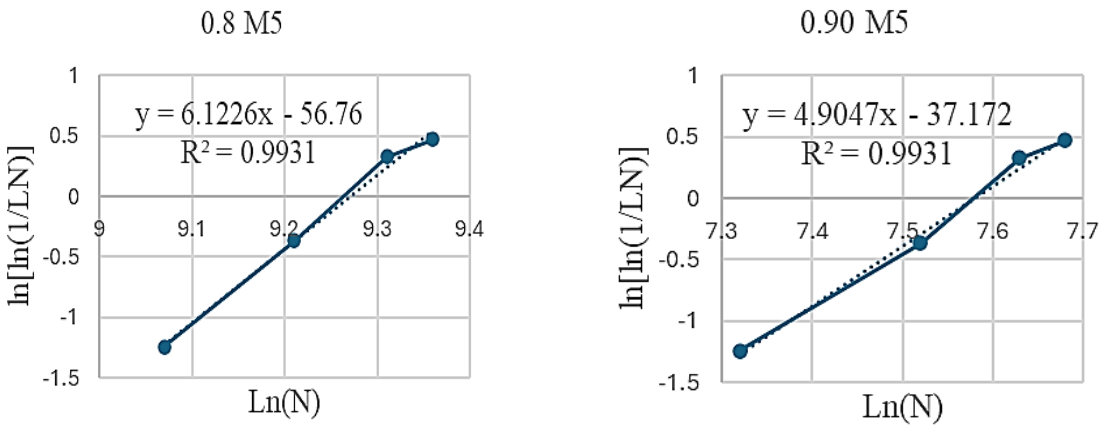
(b) M2



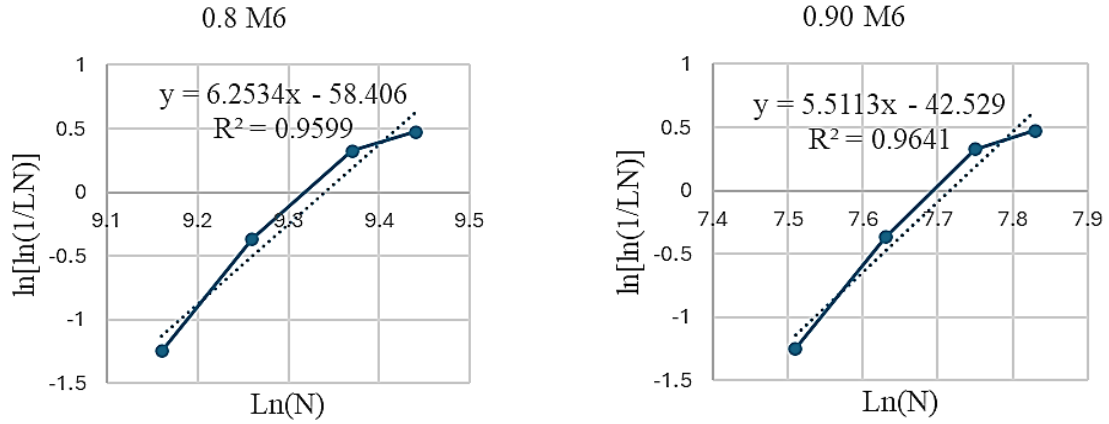
(c) M3



(d) M4



(e) M5



(f) M6

Fig. 4. Weibull plots of fatigue life data for GPC mixes (M1–M6) (a-f) at stress levels of 0.8 and 0.90 were developed using the graphical method

4.2 Weibull Distribution Parameters

The Weibull parameters for the control mix (M1) were investigated at stress levels of 0.80 and 0.90 using the graphical method, the method of moments, and their average. At a 0.80 stress level, the shape (α) and scale (U) parameters showed a similar trend of increase from M1 to M6 in all three cases. In the graphical method, an increase in α from M2 to M6 was observed in the range of 2.67% to 21.16%, and U ranged from 4.08% to 27.89%. The method of moments, the increase in α from M2 to M6 ranged from 4.62% to 24.53% and U from 3.41% to 27.31% with respect to M1. The trend was the same for the average values, showing that fatigue performance steadily improved with each mix change, with M6 showing the most improvement. When the stress level was 0.90, the shape parameter changed a little. The graphical approach indicated that M2 and M3 experienced decreases in α of 5.65% and 5.04%, respectively, while the other mixes showed increases in α, with a peak of 17.13% in M6. Similarly, under the method of moments, α decreased up to M3 and then increased by up to 15.29% at M6. However, for the scale parameter U, there was a continuous increase across all mixes in both methods. In the graphical method, U increased from 11.50% (M2) to 36.45% (M6), while in the method of moments, it increased from 9.35% to 33.87%. This was also evidenced by the average values, which showed that fatigue life could be enhanced at increased stress levels with increased mix proportions. Fatigue resistance increases with nano-silica due to pore filling, improved bonding, and denser microstructure [2,13-15]. Fatigue resistance increases with molarity due to improved geopolymerization but decreases at higher levels due to brittleness and microcracking.

Higher mix levels (M5 and M6) exhibit superior fatigue performance, indicated by increased scale (U) and improved shape (α) parameters. Fatigue resistance increases with fiber addition due to crack bridging and energy absorption [6,16,17]. The method of moments yields slightly higher values than the graphical method, suggesting more stable and conservative estimates. Overall,

modified mixes, especially M6, ensure better durability and reliability under repeated loading conditions. At a 0.80 stress level, both α and U increase consistently from M1 to M6, indicating stable and improved fatigue performance. At 0.90, α initially decreases, then increases, showing greater variability, and overall α values are lower than at 0.80, indicating greater scatter at higher stress. U increases continuously. Higher stress accelerates crack formation, causing early instability, while improved mixes enhance fatigue resistance [18,19]. The graphs are represented in Fig. 4(a–f).

5. Design Fatigue Life Estimation

To assess the reliability of the concrete mixes under repeated loading, this section aims to determine the design fatigue life (N_D) of each mix at different probabilities of failure (P_f) using the Weibull distribution parameters. The N_D value represents the estimated number of load cycles that a particular concrete mix can sustain at a specified probability of failure and stress level. Determining N_D for mixes M1–M6 enables the comparison of their fatigue life and reliability and helps identify the mixes with better performance under repeated loading. These design fatigue lives can be used to develop fatigue life curves and support pavement and structural design. Design fatigue predictions for different concrete mixes have been widely studied [9,15].

The design reliability can be expressed as, $L_N[N>N_D] = 1-P_f$, where P_f is the probability of failure.

$$N_D = u[ln(1/(1-Pf)]^{1/\alpha} \quad (9)$$

Based on the chosen probabilities of failure (P_f) of 0.01, 0.05, 0.10, and 0.20, the design fatigue life (N_D) of the concrete mixes (M1-M6) can be predicted using Equation (9). This can be calculated based on the Weibull distribution parameters (α and u) evaluated from Equations (4) and (5) at various stress levels (S). Decreasing the value of P_f (i.e., increasing the reliability) results in a shorter design fatigue life, thereby improving performance under fatigue loading. The estimated N_D values for the selected mixes at different stress levels and failure probabilities are presented in Table 7.

5.1 Design Fatigue Life (N_D)

At a stress level of 0.80, all modified mixes (M2–M6) showed a consistent improvement in N_D relative to M1 across all failure probabilities. The percentage increase ranged from approximately 1% to 20%, with higher mixes showing greater enhancement. M5 and M6 demonstrated the most significant improvement, indicating superior fatigue resistance. Fig. 5 shows the fatigue-life design for the various mixes (M1–M6). At a stress level of 0.90, a similar trend was observed, with all mixes showing improved fatigue life relative to M1. The percentage variation ranged from about 5% to 20%, with more pronounced gains at higher failure probabilities. Despite the overall reduction in absolute fatigue life at higher stress levels, the relative improvement due to mix modification was more significant, particularly for M5 and M6, confirming their enhanced performance under severe loading conditions, as reflected in the design fatigue lives presented in Table 10. The design fatigue life increased progressively from M1 to M6, with the improvement mainly associated with increased activator molarity and the incorporation of nano-silica, I-Crete, and banana fiber. At a stress level of 0.80 and a failure probability of 1%, the fatigue life increased from 3651 cycles for M1 to 3889, 4471, 4588, 5013, and 5455 cycles for M2–M6, respectively. This corresponds to an overall improvement of 49.4% for M6 compared with M1.

The increase from M1 to M3 is attributed to the rise in NaOH molarity from 8 M to 12 M, which promotes better geopolymer matrix development. The addition of 2% nano-silica in M4 produced a small improvement, while 2% I-Crete in M5 provided a further increase in fatigue life. The highest fatigue life was obtained for M6 with 2% banana fiber, which can be attributed to the fiber's crack-bridging and crack-arresting effects, delaying crack propagation under repeated loading. Overall, M6 showed the best fatigue performance among the investigated mixes. The failure probabilities of 1%, 5%, 10%, and 20% were selected to represent different levels of reliability in the fatigue-life assessment. The lower failure probabilities of 1% and 5% provide more conservative estimates of fatigue life, while 10% and 20% allow the fatigue performance of the mixes to be evaluated at relatively higher allowable failure probabilities. These reliability levels were selected to provide a

practical range for comparative assessment of the fatigue performance of the investigated mixes and to examine the sensitivity of the design fatigue life to the selected failure probability.

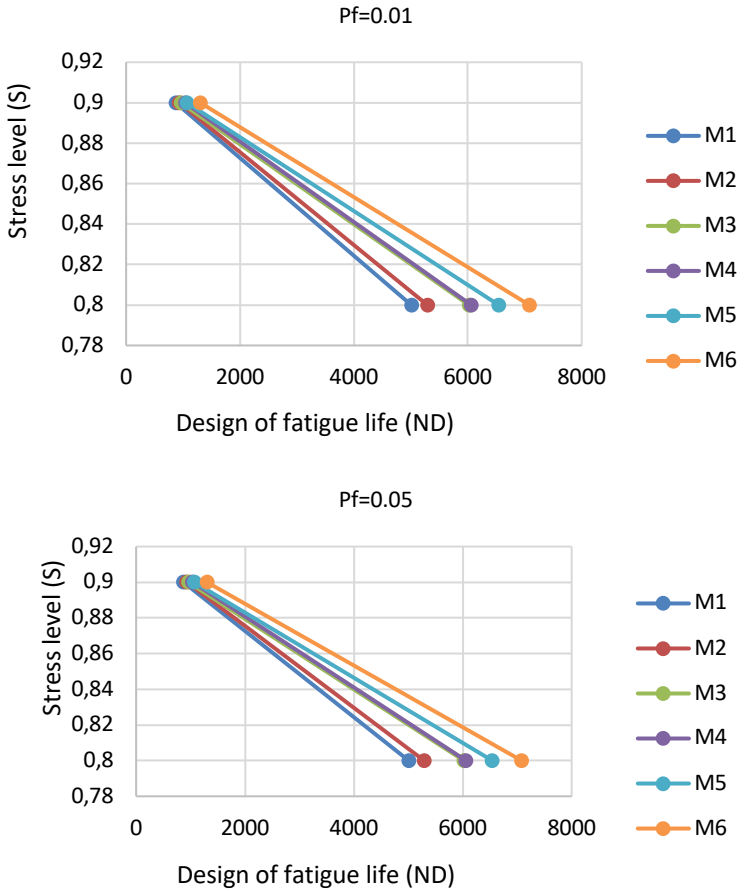


Fig. 5. Design of fatigue life for various mixes (M1-M6)

Table10. Design fatigue lives (Number of load cycles)

Mix ID	Stress level	Design fatigue lives ND = u [ln (1 / (1 - Pf)]1/α			
		P'=0.01	P'=0.05	P'=0.1	P'=0.2
M1	0.80	3651	5007	5756	6657
	0.90	615	870	1014	1189
M2	0.80	3889	5290	6060	6981
	0.90	647	934	1099	1301
M3	0.80	4471	6019	6864	7871
	0.90	666	959	1127	1334
M4	0.80	4588	6061	6854	7792
	0.90	739	1036	1202	1404
M5	0.80	5013	6542	7358	8317
	0.90	766	1068	1237	1442
M6	0.80	5455	7081	7944	8957
	0.90	969	1302	1484	1700

6. Two-Million-Cycle Endurance Limit of Different Concrete Mixes

In the present study, fatigue tests were conducted at two stress levels, namely 0.80 and 0.90 of the static flexural strength. These experimentally obtained stress levels were used to establish the S–N relationship for each mix. The S–N curves were developed by plotting the natural logarithm of the cycles to failure, Log(N), on the X-axis and the normalized stress level, S = fmax/fr, on the Y-axis.

The established S–N trends were then extended to Log(N) = 6.3, corresponding to 2 million cycles, and the stress level at this point was taken as the endurance limit. The resulting endurance limits were expressed as a percentage of the corresponding static flexural strength for comparison among the investigated concrete mixes.

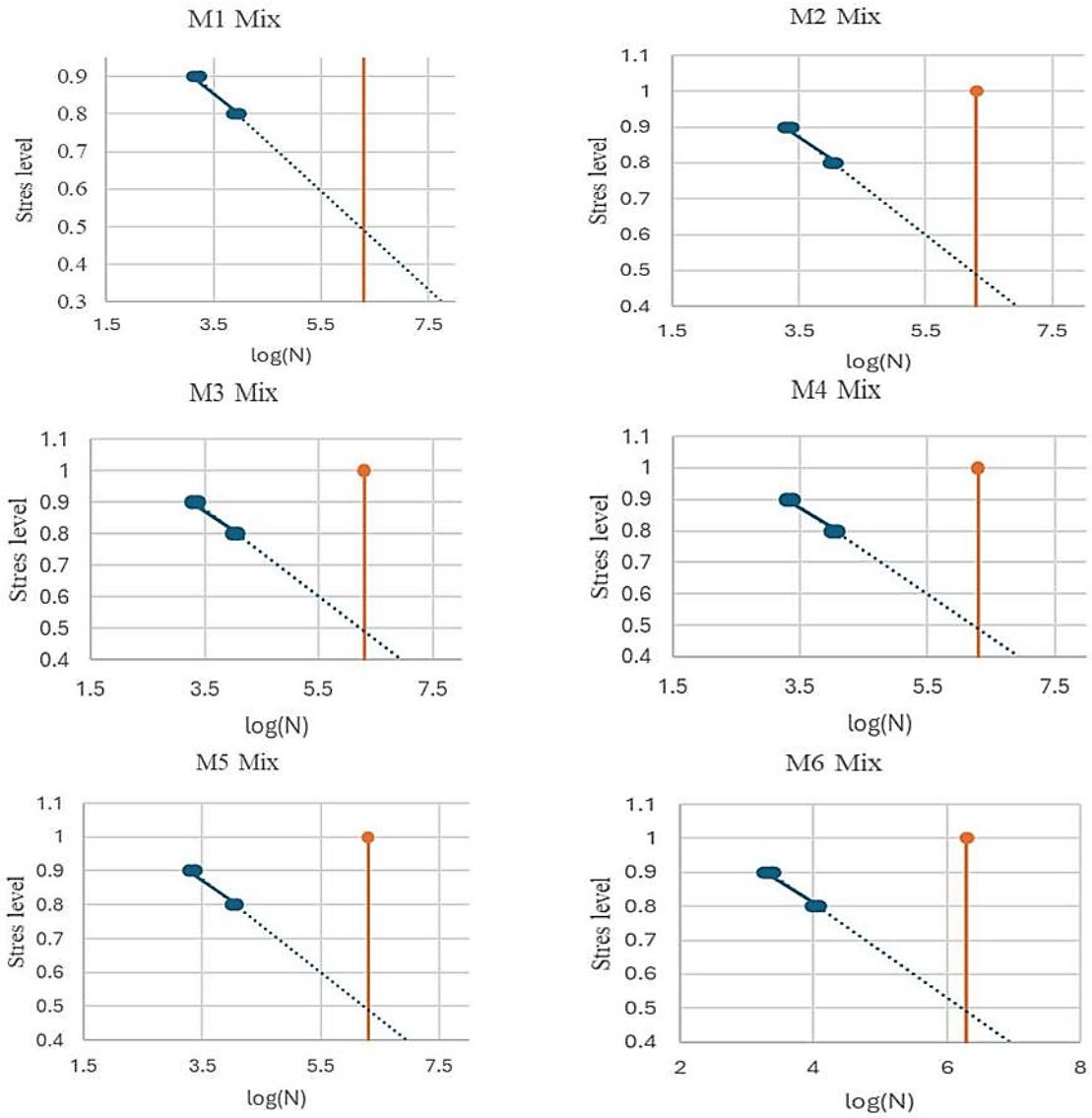


Fig. 6. Endurance limit of different concrete mixes(M1-M6)

The control mix (M1) exhibited an endurance limit of 50.0%. The mixes M2, M3, M4, M5 and M6 showed endurance limits of 49.5%, 50.5%, 50.0%, 49.0% and 50.5%, respectively. Compared with the control mix, M2 and M5 showed slight decreases of 1.0% and 2.0%, respectively, whereas M3 and M6 showed marginal increases of 1.0%, and M4 showed no variation. Overall, the endurance-limit values were closely grouped within 49.0%–50.5%, with a maximum variation of 1.5 percentage points. This narrow range indicates a consistent endurance-limit response across all investigated mixes. The small variations observed may be attributed to the inherent scatter associated with fatigue testing and specimen-to-specimen variability. The results therefore indicate that the incorporation of different constituent materials maintained a comparable endurance-limit level, while their influence may be more evident in the fatigue-life response at the selected stress levels. The fatigue results indicate that the 12 M mixes and the mixes incorporating modified binders exhibited better fatigue performance than the corresponding 8 M and 10 M mixes. The higher fatigue life observed at 12 M indicates improved resistance to repeated loading, while the modified-binder mixes further enhanced the fatigue response through their contribution to the binder matrix. Although the endurance-limit values showed a relatively narrow variation of 49.0%–50.5%, the differences in fatigue life demonstrate that the effect of molarity and binder

modification is more clearly reflected in the number of cycles sustained before failure. From a practical application perspective, the higher fatigue life of the 12 M and modified-binder mixes indicates greater suitability for concrete elements subjected to repeated or cyclic loading, as they can sustain a greater number of load repetitions before failure. Fig. 6 illustrates the endurance limit of different concrete mixes (M1–M6), highlighting minimal variation among them despite the incorporation of different materials.

7. Conclusions

- At a stress level of 0.80, the Weibull shape parameter (α) and characteristic life (U) increased progressively from M1 to M6, with maximum improvements of approximately 23% and 28%, respectively, indicating enhanced fatigue resistance.
- At a stress level of 0.90, α initially decreased in M2 and M3 but subsequently increased up to approximately 17% in M6, while U increased continuously by up to 36%, demonstrating improved fatigue-life characteristics under higher cyclic stress.
- The improvement in fatigue performance was influenced by the material modifications. Increasing NaOH molarity enhanced geopolymer matrix development, while 2% nano-silica contributed to matrix densification and pore refinement. 2% I-Crete further improved the binder matrix, whereas 2% banana fibre in M6 enhanced crack bridging and crack arresting, thereby delaying crack propagation under cyclic loading.
- The method of moments generally produced higher Weibull α and U values than the graphical method, confirming the consistent improvement in the fatigue characteristics of the modified mixes.
- The design fatigue life increased from 3651 to 5455 cycles at 0.80 stress level and from 615 to 969 cycles at 0.90 stress level, corresponding to improvements of approximately 49% and 58%, respectively. M6 exhibited the highest design fatigue life among the investigated mixes.
- The endurance limits varied only slightly, from 49.0% to 50.5% of the static flexural strength, indicating that the material modifications had a limited effect on the extrapolated endurance limit.
- Overall, the combined effects of NaOH molarity, nano-silica, I-Crete, and banana fibre enhanced the fatigue-life characteristics of GPC. M6 demonstrated the highest overall fatigue performance.

Acknowledgements

The authors express their heartfelt gratitude to the Department of Civil Engineering, Sri Venkateshwara University College of Engineering, Tirupati, for providing the necessary support and facilities to carry out this research.

References

[1] Maranan GB, Manalo AC, Benmokrane B, Karunasena W, Mendis P. Evaluation of the flexural strength and serviceability of geopolymer concrete beams reinforced with GFRP bars. Engineering Structures. 2015; 101:529-541. https://doi.org/10.1016/j.engstruct.2015.08.003

[2] Choudhary L, Sahu V, Dongre A. Mechanical investigation of high-strength sustainable ternary geopolymer concrete. SSRN. 2024. https://doi.org/10.2139/ssrn.4865246

[3] Girish MG, Shetty KK, Nayak G. Effect of slag sand on mechanical strengths and fatigue performance of paving-grade geopolymer concrete. International Journal of Pavement Research and Technology. 2025;18(3):543-560. https://doi.org/10.1007/s42947-023-00363-2

[4] Goonewardena J, Ghabraie K, Subhani M. Flexural performance of FRP-reinforced geopolymer concrete beam. Journal of Composites Science. 2020;4(4):187. https://doi.org/10.3390/jcs4040187

[5] Maaz M, Khan RA, Sharma R. Fatigue and fracture behavior of geopolymer concrete. Materials Today: Proceedings. 2023;93:163-169. https://doi.org/10.1016/j.matpr.2023.07.113

[6] Silva ACR, Almeida BM, Lucas MM, Cândido VS, da Cruz KSP, Oliveira MS, et al. Fatigue behavior of steel fiber reinforced geopolymer concrete. Case Studies in Construction Materials. 2022;16:e00829. https://doi.org/10.1016/j.cscm.2021.e00829

[7] Candido VS, da Silva ACR, Simonassi NT, Lima ES, da Luz FS, Monteiro SN. Mechanical and microstructural characterization of geopolymeric concrete subjected to fatigue. Journal of Materials Research and Technology. 2018;7(4):566-570. https://doi.org/10.1016/j.jmrt.2018.07.011
[8] Shibayama A, Nishiyama M. Flexural strength and load-deformation relationship of fly-ash-based geopolymer concrete beams. Japan Architectural Review. 2023;6(1):e12331. https://doi.org/10.1002/2475-8876.12331
[9] Liu J, Yan F. Study on the flexural behavior of reinforced concrete beams strengthened with geopolymer adhesive-bonded CFRP. International Journal of Structural Integrity. 2022;13(3):448-468. https://doi.org/10.1108/IJSI-01-2022-0009
[10] Paluri Y, Noolu V, Mudavath H, Kumar Pancharathi R. Flexural fatigue behavior of steel fiber-reinforced RAP-based concrete. Practice Periodical on Structural Design and Construction. 2021;26(1):04020053. https://doi.org/10.1061/(ASCE)SC.1943-5576.0000540
[11] Goel S, Singh SP, Singh P. Flexural fatigue analysis of self-compacting concrete beams. Proceedings of the Institution of Civil Engineers. 2012;165(6):367-376. https://doi.org/10.1680/coma.11.00016
[12] Arora S, Singh SP. Analysis of flexural fatigue failure of concrete made with 100% coarse recycled concrete aggregates. Construction and Building Materials. 2016;102:782-791. https://doi.org/10.1016/j.conbuildmat.2015.10.098
[13] Gao Y, Zhou W, Zeng W, Pei G, Duan K. Preparation and flexural fatigue resistance of self-compacting road concrete incorporating nano-silica particles. Construction and Building Materials. 2021;278:122380. https://doi.org/10.1016/j.conbuildmat.2021.122380
[14] Dong B, Liu C, Shumuye ED, Zhang Y, Zhong H, Fang G. Effect of nano-silica on mechanical properties and microstructure of engineered geopolymer composites. Cement and Concrete Composites. 2025;156:105849. https://doi.org/10.1016/j.cemconcomp.2024.105849
[15] Çevik A, Alzeebaree R, Humur G, Niş A, Gülşan ME. Effect of nano-silica on the chemical durability and mechanical performance of fly ash based geopolymer concrete. Ceramics International. 2018;44(11):12253-12264. https://doi.org/10.1016/j.ceramint.2018.04.009
[16] Barış KE, Tanaçan L. Performance of natural pozzolan-based geopolymer reinforced with banana fibers. Journal of Green Building. 2024;19(1):51. https://doi.org/10.3992/jgb.19.1.51
[17] Banjara NK, Ramanjaneyulu K, Sasmal S, Srinivas V. Flexural fatigue performance of plain and fibre-reinforcedf concrete. Transactions of the Indian Institute of Metals. 2016;69(2):373-377. https://doi.org/10.1007/s12666-015-0770-y
[18] Das A, Kumar S, Sharma P, Sharma N. Environmental effects of cement production: A review. Springer Conference Proceedings. 2022:597-608. https://doi.org/10.1007/978-981-99-1894-2_51
[19] Deivabalan B, Saravanan D. Fatigue behaviour of geopolymer concrete beam. International Journal of Research in Engineering, Science and Technology. 2015;1(6):39-45.
[20] Long T, Zhang H, Chen Y, Li Z, Xu J, Shi X, et al. Effect of sulphate attack on the flexural fatigue behaviour of fly ash-based geopolymer concrete. The Journal of Strain Analysis for Engineering Design. 2018;53(8):711-718. https://doi.org/10.1177/0309324718783607
[21] Girish MG, Shetty KK, Nayak G. Effect of slag sand on mechanical strengths and fatigue performance of paving grade geopolymer concrete. International Journal of Pavement Research and Technology. 2025;18(3):543-560. https://doi.org/10.1007/s42947-023-00363-2
[22] da Silva ACR, Almeida BM, Lucas MM, Candido VS, da Cruz KSP, Oliveira MS, et al. Fatigue behavior of steel fiber reinforced geopolymer concrete. Case Studies in Construction Materials. 2022;16:e00829. https://doi.org/10.1016/j.cscm.2021.e00829
[23] Min WL, Jin WL, He XY, Wu RJ, Chen KY, Chen JJ, et al. Experimental study on the flexural fatigue performance of slag/fly ash geopolymer concrete reinforced with modified basalt and PVA hybrid fibers. Journal of Building Engineering. 2024;94:109917. https://doi.org/10.1016/j.jobe.2024.109917
[24] Gao YX, Yi JZ, Lee PD, Lindley TC. A micro-cell model of the effect of microstructure and defects on fatigue resistance in cast aluminum alloys. Acta Materialia. 2004;52(19):5435-5449. https://doi.org/10.1016/j.actamat.2004.07.035
[25] Bureau of Indian Standards (BIS). IS 383:2016 - Coarse and fine aggregate for concrete - specification, fifth revision. New Delhi: BIS; 2016.
[26] Indian Roads Congress (IRC). IRC:58-2015 guidelines for the design of plain jointed rigid pavements for highways. New Delhi: IRC; 2015.